

Objective, observations-based, automatic estimation of the catchment response timescale

Efrat Morin,¹ Konstantine P. Georgakakos,^{2,3} Uri Shamir,⁴ Rami Garti,⁵ and Yehouda Enzel⁶

Received 30 July 2001; revised 10 April 2002; accepted 15 May 2002; published 24 October 2002.

[1] A new characteristic timescale of a catchment is presented, the response timescale (RTS). It is a range of averaging time intervals which, when applied to catchment rainfall, yield smoothed time series that best approximate that of the resultant runoff. In determining the RTS, nothing is assumed about the nature of the rainfall-runoff transformation. In addition, this new measure is shown to be robust against measurement errors. An objective, automatic, observations-based algorithm is described that introduces the concept of peaks density for the estimation of RTS. Estimation is exemplified for single and multiple rainfall-runoff events through application to small catchments in Panama and Israel. In all cases, relatively stable values of response timescale are obtained. It is concluded that at least for the case studies, the response timescale is an intrinsic characteristic of the catchment and it is generally expected to be different from the catchment lag time and time of concentration. *INDEX TERMS:* 1854 Hydrology: Precipitation (3354); 1860 Hydrology: Runoff and streamflow; 3360 Meteorology and Atmospheric Dynamics: Remote sensing; *KEYWORDS:* characteristic timescale, catchment hydrology, hydrological response, rainfall-runoff relationships, meteorological radar, small basins

Citation: Morin, E., K. P. Georgakakos, U. Shamir, R. Garti, and Y. Enzel, Objective, observations-based, automatic estimation of the catchment response timescale, *Water Resour. Res.*, 38(10), 1212, doi:10.1029/2001WR000808, 2002.

1. Introduction

[2] The hydrological response of a catchment is a composition of different processes with a variety of characteristic timescales. Associating the catchment response, as a whole, with one representative characteristic scale is important in many aspects of hydrology, both theoretical, for better understanding the integration of the different processes for the production of runoff and streamflow, and practical, for modeling and design purposes. The goal of this paper is to present a new characteristic timescale of a catchment, the Response Timescale (RTS), and to outline an objective, observations-based, algorithm to determine this scale.

1.1. Literature Review

[3] Several different characteristic timescales have been suggested in the literature. One of the most commonly used is the time of concentration, which is defined as the time required for a drop of water falling on the most remote part

of the catchment to reach its outlet. According to its definition, the time of concentration can only be attained if all initial losses are satisfied and uniform rainfall continues over the entire catchment for a period at least equal to the time of concentration; situations that are very rare in natural conditions [Singh, 1992]. To allow a practical use of this parameter, different experimental and theoretical studies were conducted to obtain formulas that associate it with catchment characteristics, such as catchment length and slope [e.g., Kirpich, 1940; Soil Conservation Service, 1972]. Some of the studies show that the time of concentration is also a function of rainfall characteristics [Singh, 1976; Ben-Zvi, 1984].

[4] Another widely used time parameter is the lag time, defined as the time elapsed between the center of mass of effective rainfall and the center of mass of the direct runoff hydrograph. Sometimes the peak of the direct runoff hydrograph is used instead of the center of mass, because of the difficulty in determining the latter. In an extensive study, Simas and Hawkins [1998] evaluated lag time for over 50,000 rainfall-runoff events in 168 small catchments (smaller than 15 km²) in the United States. They observed a stable value of lag time for the larger storms, with the peak flow as the hydrologic variable that best showed this tendency. A similar conclusion was reached by Caroni *et al.* [1986], who found that the nonlinearity in the rainfall-runoff transformation is decreased with increasing storm intensity. Linear relationships were suggested between lag time and time of concentration by Soil Conservation Service [1975], Overton and Meadows [1976] and others. Additional time parameters are suggested in the literature such as the risetime, defined as the time elapsed from the beginning

¹Department of Hydrology and Water Resources, University of Arizona, Tucson, Arizona, USA.

²Hydrologic Research Center, San Diego, California, USA.

³Also at Scripps Institution of Oceanography, University of California, San Diego, La Jolla, California, USA.

⁴Faculty of Civil Engineering and Stephen and Nancy Grand Water Research Institute, Technion, Haifa, Israel.

⁵Soil Erosion Research Station, Emek Hefer, Israel.

⁶Institute of Earth Sciences, Hebrew University of Jerusalem, Jerusalem, Israel.

of the rising limb to the peak discharge, time to equilibrium, which is time elapsed before there is no significant difference between inflow and outflow, and volume/peak ratio [Bell and Om Kar, 1969].

[5] Time characteristics are a central part of hydrologic modeling and design. Almost all hydrological models contain at least one time parameter. For instance, the simple linear reservoir model [Singh, 1992] has a single parameter, the storage parameter, which has dimensions of time and it is equal to the first moment of the Instantaneous Unit Hydrograph (IUH). The frequently used Nash model [Nash, 1959], a cascade of equal linear reservoirs, contains an additional parameter, the number of reservoirs. The lag time of the whole series of reservoirs becomes the product of the number of reservoirs and the storage parameter. In representing the concept of the geomorphologic IUH, Rodriguez-Iturbe and Valdes [1979] link the structure of the catchment hydrological response to its geomorphologic parameters, namely the Horton ratios [Horton, 1945]. In addition to the Horton ratios, characteristic length and velocity parameters are used to construct the instantaneous unit hydrograph; the ratio of these two represents a characteristic time parameter. This time parameter as well as the Horton ratios are used in determining the peak and the time to peak of the geomorphologic IUH. Another example of the importance of characteristic timescales in hydrological applications is the rational formula [Kuichling, 1889], for which the peak discharge is proportional to the rainfall intensity for duration longer than the time of concentration.

[6] In design flood estimation characteristic response times are required for the determination of hydrograph parameters and critical durations of flood-producing rainfall. Bell and Om Kar [1969] compared the use of some of the above characteristic timescales in design flood estimations. They found the risetime and volume/peak ratio to be too dependent on storm characteristics and suggested the critical-lag time parameter as the most appropriate for design purposes. The critical-lag is defined as the average value of lag time for extreme floods (return periods greater than 10 years). The importance of the catchment characteristic timescale in flood frequency analyses is further demonstrated by Robinson and Sivapalan [1997]. The authors examined the interaction between catchment response time and two rainfall characteristic timescales, storm duration and inter arrival period, and their effect on flood frequency parameters. They defined five hydrological regimes according to the relationships between the three time parameters and constructed flood frequency curves for each regime using a linear rainfall-runoff model and synthetic rainfall. They show that within-storm patterns have the biggest impact in fast regimes while multiple storms and seasonality have the biggest impact in slow regimes. The characteristic response time is also central in the paper of Iacobellis and Fiorentino [2000]. In their study the peak discharge is expressed as a product of two random variables, the average runoff per unit area and the peak contributing area. The distribution of the first variable, for a given contributing area, is related to the rainfall depth occurring with duration equal to a characteristic response time of the contributing part of the catchment. The authors assume a power law relationship between the contributing area and the characteristic response time of this area. Michaud et al. [2001]

studied the regional variations of floods in small catchments in the United States. They identified a different response of small catchments in the semiarid west as compared with the response of small catchments in humid areas. In the first group, floods can be caused by as little as 5–10 cm of rain in 30–60 min, whereas in the second, floods result from 13–32 cm of rain falling in 1–12 hours.

1.2. Response Timescale

[7] The concept of the response timescale was first introduced by Morin et al. [2001]. In that paper, the RTS was defined as the timescale for which the pattern of the time-averaged rainfall graph is most “similar” to the pattern of the measured outlet hydrograph. Similarity there referred to the smoothness of the two graphs. At small timescales, the rainfall graph is noisy and “peaky” relative to the runoff hydrograph. As rainfall data are averaged over increasingly larger timescales, the pattern of the resulting graph becomes smoother. At large timescales, the rainfall graph pattern appears much smoother than the pattern of the runoff graph. The method for determining RTS identifies the point at which the appearance of the two graphs is most similar. Morin et al. [2001] present a heuristic procedure to estimate the RTS, which is based on associating rainfall and runoff peaks and selecting the timescale for which the number of peaks in the two graphs is the same. Rainfall peaks preceding the beginning of flow and peaks that are lower than a defined threshold were excluded from the analysis.

[8] The algorithm was applied to four studied catchments in Israel and their RTS values were identified. In general, the suggested method was found to be reliable and robust, but some difficulties were encountered, which could limit its general use. The main drawbacks are subjectivity in the peak association process and in the threshold determination; inadequate performance for events with widely separated hydrographs (typical for arid basins); and a tedious manual estimation process because of errors in the runoff data timing.

[9] In the current paper, a different definition is given to the RTS, to emphasize that the smoothness of the rainfall and runoff graphs is examined, rather than the general appearance. An objective, automatic estimation algorithm is outlined that overcomes most of the difficulties described above. The algorithm is applied to the same four semi-arid catchments observed by radar and analyzed by Morin et al. [2001] as well as to a small tropical catchment in Panama observed by recording rain gauges. The large data set of rainfall-runoff events available for the latter catchment allows examination of the dependence of the RTS uncertainty on the number of events used in the analysis and on data errors. The current paper demonstrates that the estimation algorithm exhibits the desirable property of being robust against errors in rainfall and runoff data.

[10] It is important to associate the response timescale with a hydrologic characteristic and to specify the differences between this parameter and other known time parameters. In the rainfall-to-runoff transformation and routing of water toward the catchment outlet two characteristic timescales can be identified: (1) the integration time and (2) the translation time. The first represents the generation of runoff peaks from noisy rainfall, while the latter represents the time it takes the runoff peaks to reach the catchment outlet.

If one accepts this view, then the response timescale can be associated with the integration time, while the lag time can be associated with the translation time. The time of concentration is a combination of these two. The two time characteristics are not necessarily related. For example, a catchment that has a short integration time, i.e., its runoff hydrograph is relatively close in its smoothness to the rainfall hyetograph, may have a relatively long translation time. Such an example is shown in this paper for one of the studied catchments. The presented study deals with the identification, stability and robustness of the response timescale and its algorithm. In this first step we use an observations-based (rather than model based) approach to derive this characteristic scale, in order to minimize the influence of a hydrological model and its parameters on our results. In ongoing research, the other approach is used to study the physical interpretation of the response timescale and the scale sensitivity to catchment observable geomorphological characteristics.

1.3. Organization of the Paper

[11] Section 2 describes the study catchments (in Panama and Israel) and the data used for the analysis. The concept of the response timescale and the algorithm for its estimation are described in section 3. In section 4, the algorithm is exemplified by way of application to the Habel catchment. In the same section, insensitivity to linear and nonlinear changes in rainfall and runoff is demonstrated. The application of the algorithm to the rest of the catchments is described in section 5. Discussion and concluding remarks are in sections 6 and 7, respectively.

2. Catchments and Data

2.1. Panama Catchment

[12] The Rio Pequeni is a 133-km² catchment in the northeastern sector of the Panama Canal Watershed in the tropics (coordinates 79.4° W, 9.4° N). It has steep slopes and is largely forested. The wet season is in October–January with maximum rain amount in November in excess of 500 mm/month. The migration of the Inter Tropical Convergence Zone and pronounced orographic effects make for intense convective rainfall in the catchment [Georgakakos *et al.*, 1999].

[13] Rainfall and runoff data for the Rio Pequeni catchment are available for the years 1972–1996. Out of the 666 rainfall-runoff events determined for this period, 190 events for which the runoff peak was above 100 m³ s⁻¹ were selected for the analysis (the highest discharge recorded for this period was 1100 m³ s⁻¹). The rainfall data used in the analysis are hourly mean areal precipitation (MAP) estimated using U.S. National Weather Service (NWS) operational methods for precipitation in mountainous terrain [Georgakakos *et al.*, 1999]. The MAP data are calculated based on four automated gauges (two are in and two near the catchment). Hourly streamflow data are obtained from a recording gauge at the catchment outlet. Figure 1 shows the Rio Pequeni catchment and gauges.

2.2. Israeli Catchments

[14] Four small catchments (10–100 km²) in the semi-arid and arid regions of Israel were selected as case studies.

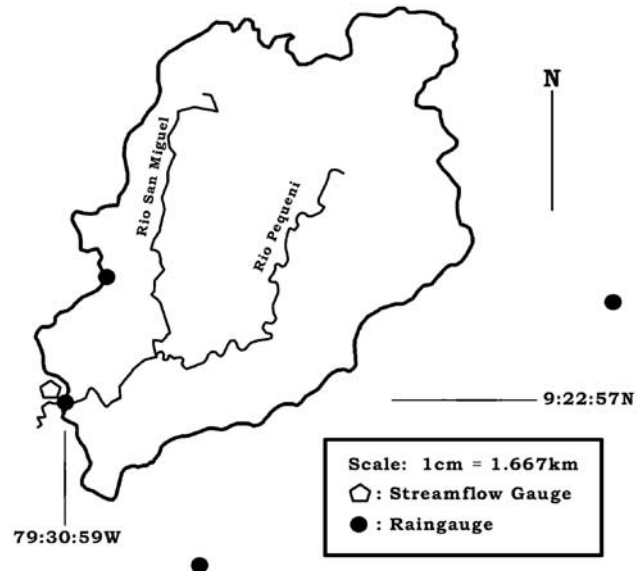


Figure 1. Map of Panama catchment and gauges.

The catchments have different size, land-use, soil type, and climatic regime: Raanana is a 10 km² urban catchment; Habel and Evtach are rural catchments with sizes of 24 km² and 43 km², respectively; Ramon is an arid catchment, of 98 km². Figure 2 represents the location and boundary of the catchments. Table 1 specifies some of the catchments main characteristics. In all the four catchments surface water is the primary source of runoff. For each catchment few storms were selected for the analysis. Table 2 lists the storms dates and total depth (storm depth was derived from a daily rain gauge located in or near the catchment).

[15] Rainfall data are MAP calculated from radar rainfall. The C band meteorological radar system is located at Ben-Gurion Airport near Tel-Aviv (see Figure 2). The spatial resolution of the radar data is 0.5–4 km² (depending on the distance from the radar system) and the temporal resolution is 5 minutes. Reflectivity data were transformed into rain intensities by using the power law equation [Marshall and Palmer, 1948]:

$$Z = 200 * R^{1.6} \quad (1)$$

where Z is the reflectivity in mm⁶m⁻³, and R is the rain intensity in mm/h. An adjustment to gauge data was applied to the data because it does not affect the estimated RTS as is shown in Section 4 below. The quality of the radar data is comparable to that of other radar systems in the world that have the same configuration. Relatively large uncertainty is associated with rainfall intensities estimated from radar reflectivities [e.g., Austin, 1987]. This uncertainty affects mainly the magnitude of the rainfall graphs. Examination of the data did not indicate any type of errors that could affect the smoothness of the radar-based rainfall graph, such as anomalous propagation or internal noise.

[16] Runoff data were obtained from two types of instruments: (1) an analog water level continuous recorder and (2) a digital instrument, which measures and logs pressure every 5 minutes. The instrument is located near channel bottom, and the recorded pressure is transformed into water

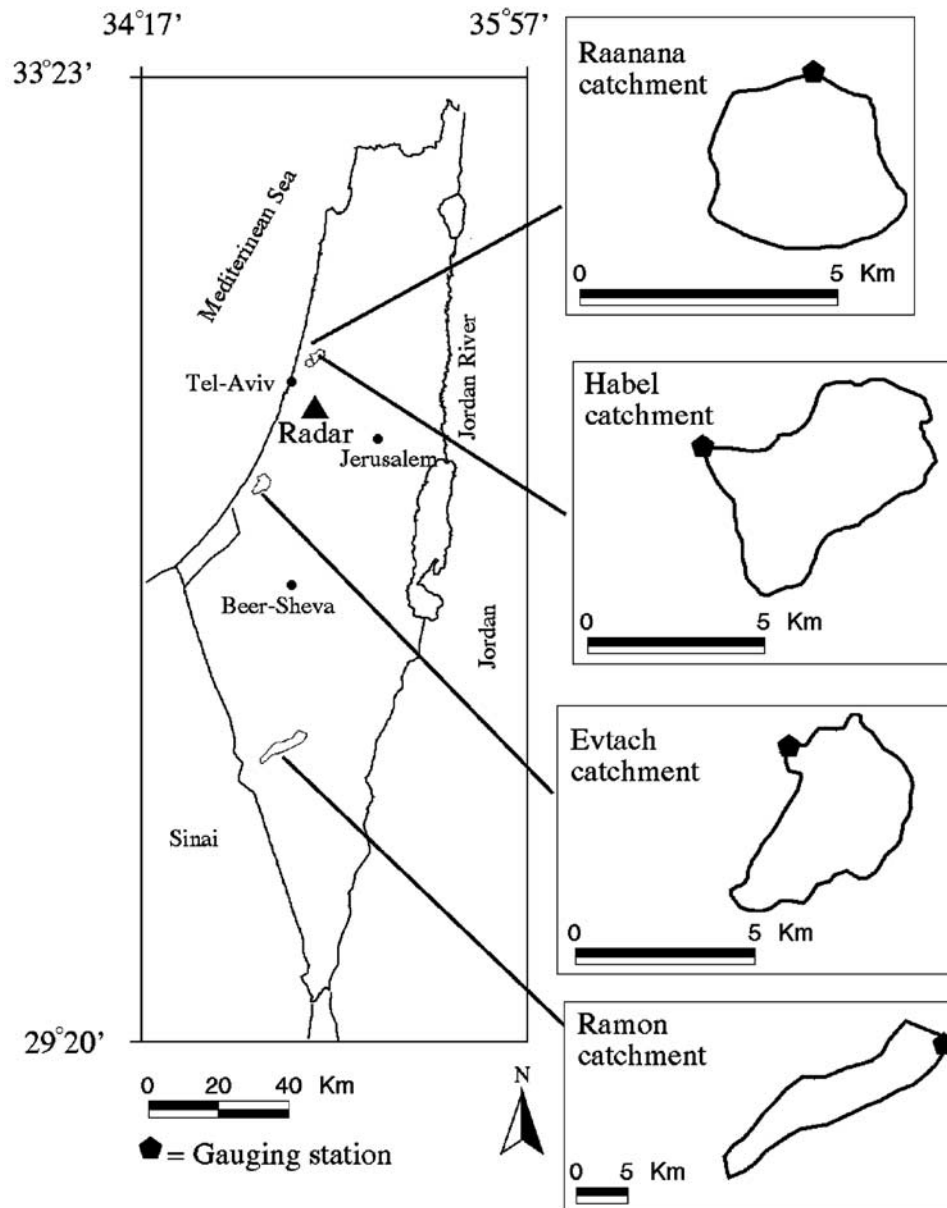


Figure 2. Map of Israeli catchments and radar.

level. An important advantage of the digital logger is its accuracy in time, which may not be the case for the analog instrument. An analog gauge was used for the Evtach and the Ramon catchments, while a digital gauge was used for the Raanana catchment. Two of the three events in the

Habel catchment were measured with the analog instrument and one event was measured with the digital instrument. Discharge is estimated from water level data using a stage-discharge curve. The graphs of runoff presented in this study are in terms of either discharge or stage, depending on

Table 1. Israeli Catchments Characteristics

Name	Size, km ²	Annual Rain Depth, mm/yr	Relief Ratio ^a	Main Channel Slope	Main Channel Length, km	Drainage Density, ^b m ⁻¹	Land Use	Dominant Soil Type ^c
Raanana	10	600	0.0089	0.009	3.5	0.0100 ^d	urban	E
Habel	24	600	0.0111	0.007	7.1	0.0007	rural	E
Evtach	43	460	0.0079	0.004	10.6	0.0015	rural	K
Ramon	98	80	0.0197	0.011	27.4	0.0038	natural	Y

^aMaximum relief divided to main channel length.

^bTotal stream length divided to catchment area.

^cE, Hamra soils; K, dark brown soils; Y, Reg soils and coarse desert alluvium [Dan and Raz, 1970].

^dEstimated value.

Table 2. Event Parameters for the Four Studied Catchments in Israel

Date	Catchment	Measured Storm Depth, mm	Measured Runoff Depth, mm	Measured Peak Discharge, cm
17–20 January 1996	Habel	191	23	22.1
22–23 January 1997	Habel	88	19	25.4
21–24 February 1997	Habel	174	40	23.9
22 February 1997	Raanana	68	NA	NA
17 March 1997	Raanana	32	NA	NA
30 November 1997	Raanana	27	5	24.0
24–25 January 1998	Raanana	27	9	8.2
17–19 March 1998	Raanana	93	26	17.7
29–30 March 1998	Raanana	11	7	13.6
30 November to 5 December 1991	Evtach	277	190	46.1
11–16 December 1991	Evtach	159	103	42.2
2–11 February 1992	Evtach	136	96	41.0
22–28 February 1992	Evtach	75	19	22.6
23–25 November 1994	Evtach	138	22	24.0
2–6 December 1994	Evtach	63	12	19.6
18–22 December 1994	Evtach	68	9	15.6
13 October 1991	Ramon	12	4	67.6
2–7 November 1994	Ramon	43	4	47.4
8 February 1996	Ramon	18	4	72.6

NA – Information is not available.

the best data available. Although the two representations of the runoff might have some differences in pattern as a result of the nonlinear transformation linking them, the number of peaks is the same in both representations.

[17] The selected events for the analysis are those that have the most reliable and consistent data. Still, some difficulties with the observed data occasionally exist, which increase the uncertainties associated mainly with the magnitude and timing of the runoff hydrographs and the rainfall graphs. However, the effect that these uncertainties have on the analysis results is believed to be insignificant in the current study, since the focus is on the smoothness of the graphs rather than on their magnitude or exact time. Section 4 discusses and demonstrates the effect of uncertainties in rainfall and runoff data on the estimated RTS.

3. Response Timescale (RTS) Concept and Algorithm

[18] Consider a general system that receives an input time series and generates an output time series. One can characterize the timescale of the system by measuring the amount of smoothing that is performed on the input in this transformation. A possible way to obtain this measure is to compare the input time series, smoothed over different timescales, with the corresponding output time series, and to select the timescale that generates a similar measure of smoothness for the two series. Thus the characterization involves analysis of the two time series, without assuming a specific model for representing the system. For a system that represents the catchment hydrological response, application of this approach implies analysis of rainfall and runoff time series. The resulting timescale is defined as the Response Timescale (RTS) of the catchment. Figure 3 shows a schematic presentation of the concept. The term “scale” is used here because the aforementioned analysis results in a relatively coarse, but stable, range of times,

rather than a very precise time value that is different for different events.

[19] This section presents an objective, automatic algorithm to determine the RTS for a given catchment on the basis of observed data. The algorithm can be applied to a single rainfall-runoff event or to a group of events. A detailed example demonstrating the application of the algorithm is given in the following section.

[20] The smoothness of the graphs is measured by the “peaks density” (*PD*) parameter, which is defined as the ratio of total peaks number (*TPN*) to the total rising limbs duration (*TRLD*):

$$PD = \frac{TPN}{TRLD} \quad (2)$$

[21] The RTS algorithm determines the peaks of a rainfall or runoff graph using a noise parameter, which is used to separate, on average, what might be called “real” increases and decreases in the graph from oscillations that are merely noise in the data. For each peak, the duration of its rising limb is determined. The total number of peaks in the graph (*TPN*) is divided by the sum of the peaks’ rising limb durations (*TRLD*) to get the *PD* of the graph. Values for the

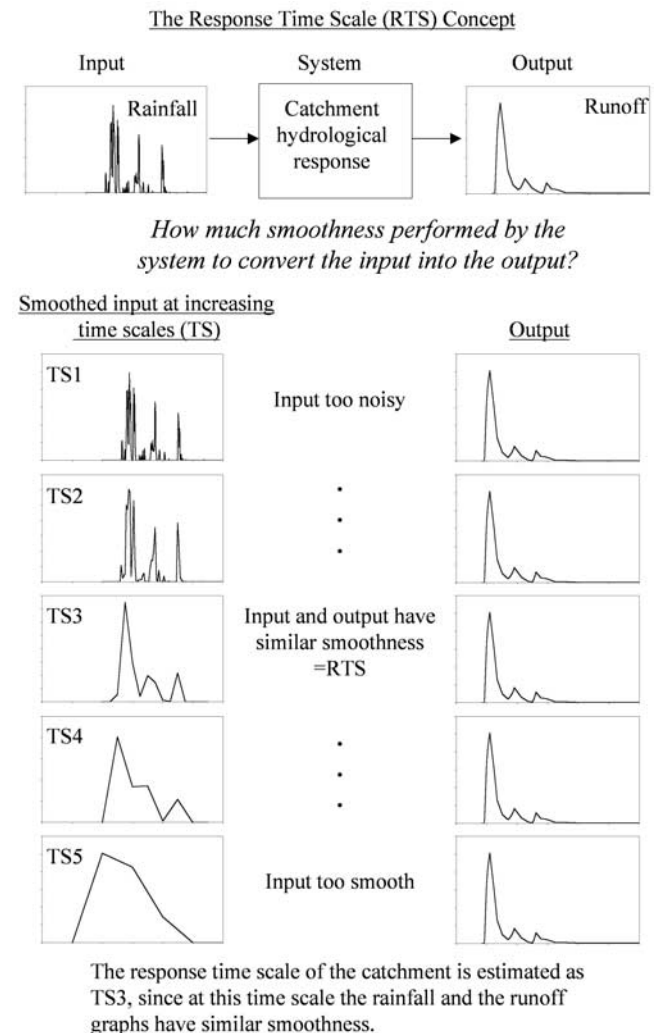


Figure 3. Scheme of the RTS concept.

noise parameter are assigned automatically in the procedure for calculating the PD of a given graph. This procedure is described in detail in Appendix A.

[22] Consider rainfall and runoff graphs of a specific rainfall-runoff event. The PD of the rainfall data is determined for different timescales. The smallest timescale that the graph can be represented is the measurement timescale. Larger timescale graphs are generated by smoothing the rainfall graph using arithmetic averaging. For each timescale, T_s , the peak density of the rainfall graph, $PD(T_s)$, is obtained. For the runoff hydrograph, the PD is determined at the measurement timescale.

[23] Viewing the PD of the rainfall as a function of the timescale of averaging, we expect it to be large for small timescales and to decrease as the timescale increases, crossing at some point the value of PD obtained for the runoff hydrograph. The timescale at which this crossover occurs is selected as the RTS of the event. In practice, the PD is not necessarily a purely monotonic function of timescale, and may include some perturbations. Therefore the range of times for which there is crossover between rainfall PD s and the runoff PD is defined as the RTS of the examined event.

[24] For a group of events, the RTS is obtained using the average of the PD values over the individual events. In addition, a range of timescales is determined, which represents one standard deviation uncertainty in the PD of the rainfall and runoff graphs. The average and standard deviation (using the $\sum_{i=1}^n PD_i / (n - 1)$ estimation, where n represents the number of events) are calculated for the rainfall at each timescale and for the runoff at the measurement scale. The RTS is defined as the range of timescales for which there is a crossover between the average rainfall PD s and the runoff PD . The uncertainty range of RTS is defined as the range of timescales for which the (rainfall average $PD \pm$ standard deviation) brackets the (runoff $PD \pm$ standard deviation). The detailed definition is as follows.

[25] Let T_{s_i} be a test timescale, H the group of events, $PD_h^R(T_{s_i})$ the peak density of rainfall for event $h \in H$ averaged at timescale T_{s_i} , and PD_h^D the peak density of the runoff for event $h \in H$. The uncertainty range of RTS for the group of events is from T_{s_L} to T_{s_U} , such that:

$$\begin{aligned} & \text{Avg}_{h \in H} (PD_h^R(T_{s_{L+1}})) - \text{Std}_{h \in H} (PD_h^R(T_{s_{L+1}})) \leq \text{Avg}_{h \in H} (PD_h^D) \\ & + \text{Std}_{h \in H} (PD_h^D) \end{aligned}$$

and for all $i \leq L$

$$\begin{aligned} & \text{Avg}_{h \in H} (PD_h^R(T_{s_i})) - \text{Std}_{h \in H} (PD_h^R(T_{s_i})) > \text{Avg}_{h \in H} (PD_h^D) + \text{Std}_{h \in H} (PD_h^D) \end{aligned} \quad (3)$$

and

$$\begin{aligned} & \text{Avg}_{h \in H} (PD_h^R(T_{s_{U-1}})) + \text{Std}_{h \in H} (PD_h^R(T_{s_{U-1}})) \geq \text{Avg}_{h \in H} (PD_h^D) \\ & - \text{Std}_{h \in H} (PD_h^D) \end{aligned}$$

and for all $i \geq U$

$$\text{Avg}_{h \in H} (PD_h^R(T_{s_i})) + \text{Std}_{h \in H} (PD_h^R(T_{s_i})) < \text{Avg}_{h \in H} (PD_h^D) - \text{Std}_{h \in H} (PD_h^D).$$

[26] These equations determine the time span during which the bandwidth (average plus and minus standard

deviation) of the smoothed rainfall is within the equivalent bandwidth of the runoff. The larger the group of events is, the better the resulting RTS represents the timescale of the catchment hydrological response. The variability of the individual events RTS, as well as the range of the RTS determined for the whole group ($T_{s_U} - T_{s_L}$), indicate the stability of the RTS parameter within the group.

[27] Section 4 below describes in detail the application of the RTS algorithm to one of the study catchments. Before that, several remarks should be made regarding the RTS algorithm:

1. The RTS algorithm in the current study is applied to the mean areal rainfall of a catchment. Use of the whole catchment as the spatial scale may affect the smoothness of the rainfall graphs and therefore also the resulting RTS. However, since the studied catchments are relatively small (10–150 km²), this effect is not significant, as is demonstrated in the next section. On the other hand, the “lumped” approach allows us to separate the timescale issue from the spatial scale issue.

2. The RTS algorithm was designed such that there is no importance to the height of the peaks, their units or their structure. Therefore any manipulation of the data that changes the peaks magnitude or shape, as long it retains the number of peaks and the duration of their rising limb, will not affect significantly the resulting RTS. This holds for the transformation of radar reflectivity data to rainfall intensities, as well as the transformation of runoff stage to runoff discharge.

3. A clarification has to be given regarding the use of the time of the rising limb of the hydrograph in the definition of the $TRLD$ parameter. The reason for considering only the rising limb duration rather than the whole hydrograph duration is that for runoff hydrographs the rising limb is the rainfall driven part of the peak. The decaying part of the runoff peak is usually slower and represents the efficiency of the catchment in draining out the runoff after the rainfall has stopped. Although the two limbs are not independent, and both contain information about the timescale characteristics of the catchment, for the purpose of this research, we concentrate on the rising limb only.

4. The measurement timescales of the rainfall and the runoff data represent the lowest limit to the determined RTS. If the RTS is found to be significantly larger than the measurement timescale then it is reasonable to assume that the latter has no effect on the RTS. Otherwise, some interaction between the two is possible and caution must be exercised in interpreting the results in such cases.

4. Example of Application

[28] In this section the application of the RTS algorithm is described in detail for the Habel catchment. The stability of the determined RTS against changes in some factors is also demonstrated. Following that, in the next section, the algorithm is applied to all five studied catchments.

[29] Rainfall and runoff data of three events in the Habel catchment are selected (see Table 2). For each event, Figures 4–6 present the rainfall graph at timescales of 5, 30, 60, 180 and 360 min (Figures 4a–4e, 5a–5e, and 6a–6e) and the measured runoff hydrograph (Figures 4f, 5f, and 6f). The rainfall data are catchment averaged radar rainfall intensities. The runoff data are discharges at the catchment

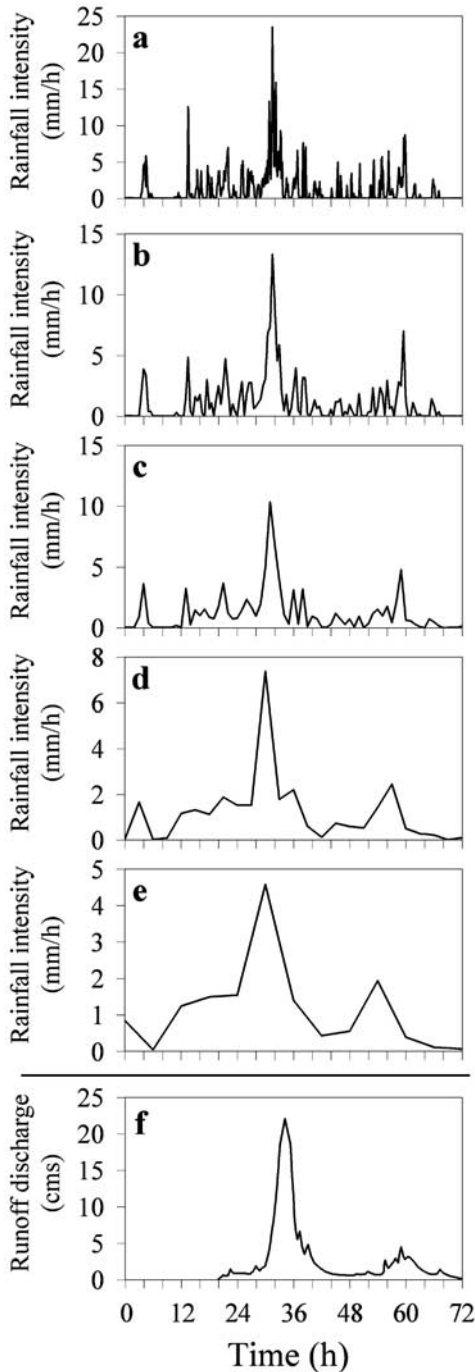


Figure 4. Rainfall and runoff graphs for the event of 17–20 January 1996 in the Habel catchment. Rainfall graphs are catchment averaged at timescales of (a) 5 min, (b) 30 min, (c) 60 min, (d) 180 min, and (e) 360 min. (f) The runoff hydrograph.

outlet. The 5-min rainfall graphs represent the rainfall at the smallest scale available (the measurement timescale). Clearly, these 5-min rainfall graphs are much noisier than the runoff graphs. The rainfall graphs at the larger timescales are created by averaging the 5-min data, which results in increasingly smoother graphs. At 360 min the rainfall graphs are already too smooth, when compared with the runoff hydrograph. Subjective inspection of the rainfall and

runoff graphs suggests that the appropriate averaging timescale is in the range of 60–180 min. Application of the RTS algorithm determines this timescale objectively.

[30] The RTS algorithm is applied for each of the events separately and for the whole group of events. The test timescales are 5–360 min in 5-min steps. Figure 7 presents the application of the RTS algorithm to the event of 17–20 January 1996. The PD of the runoff hydrograph is 0.00487 peaks/min. The PD of the rainfall graph at a 5-min timescale is 0.03691 peaks/min, and the rainfall PD generally decreases as the timescale increases. The PD of the rainfall

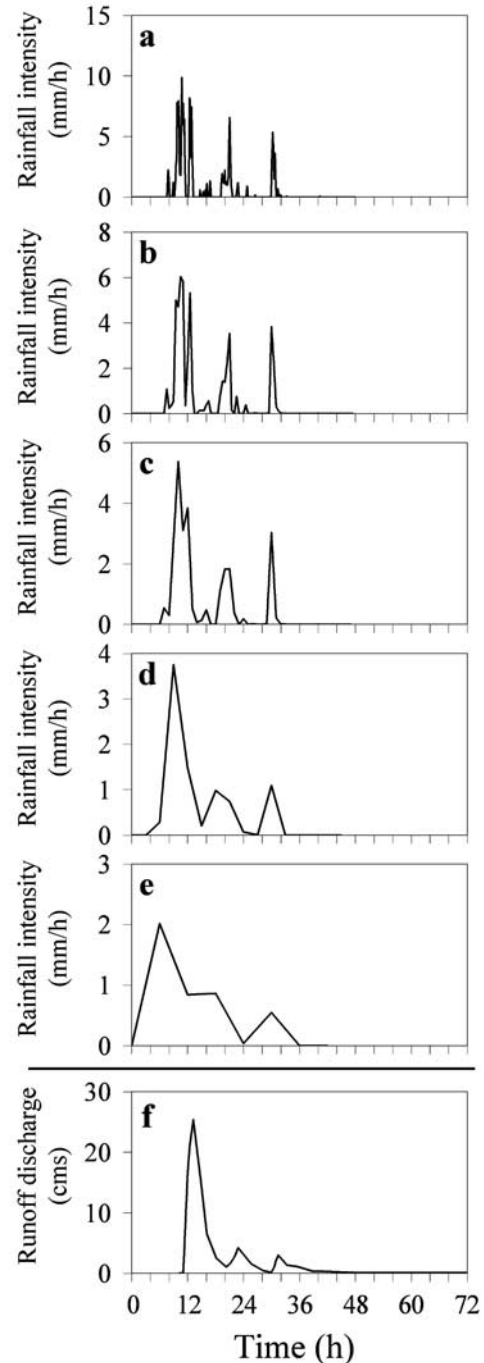


Figure 5. Same as Figure 4 for the event of 22–23 January 1997.

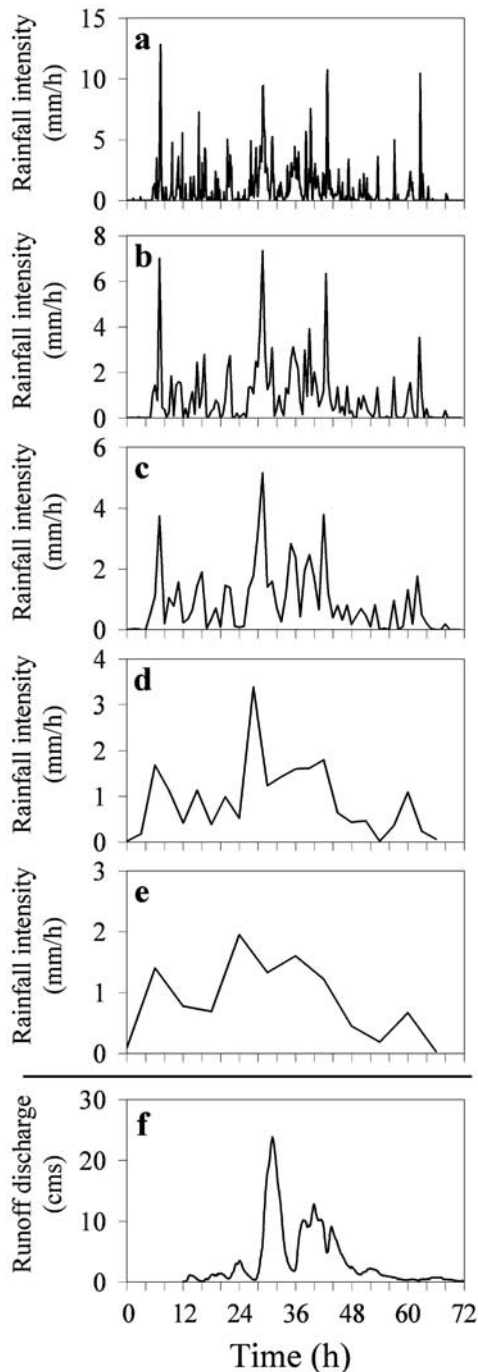


Figure 6. Same as Figure 4 for the event of 21–24 February 1997.

at timescales 5–85 min is higher than the PD of the runoff hydrograph. For timescales 90–120 min the rainfall PD is sometimes higher and sometimes lower than the runoff PD and then it stays lower for all timescales in the range 125–360 min. The range 85–125 min brackets the cross-over region of the rainfall and runoff PD graphs. It was selected as the RTS of this event. Figures 8 and 9 present the application of the RTS algorithm for the two other events. The resulting RTS values for the three events are (1) 17–20 January 1996 (Figure 7): 85–125 min; (2) 22–23 January 1997 (Figure 8): 60–85 min; (3) 21–24 February 1997 (Figure 9): 85–115 min.

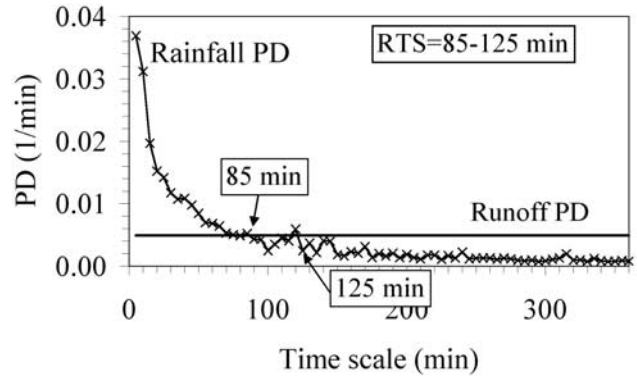


Figure 7. Application of the RTS algorithm to the Habel event of 17–20 January 1996. The PD of rainfall for timescales of 5–360 min (in 5 min steps) compared with the PD of the runoff hydrograph at the measurement scale (drawn as a constant value line). The timescale at which the rainfall PD curve crosses over the runoff curve is 85–125 min and is the selected RTS of the event.

[31] Application of the RTS algorithm for the group of the three events is shown in Figure 10. The average and the standard deviation of the PD over the three events are calculated for the observed runoff hydrograph, and for the rainfall graph at each one of the averaging timescales 5–360 min. The average PD of the rainfall crosses over the average PD of the runoff at timescales 70–85 min, which is the selected RTS for the group of events. For all the tested timescales in the range of 5–60 min the (rainfall average $PD \pm$ standard deviation) values do not overlap with the (average PD of the runoff \pm standard deviation) values. Similarly, there is no overlap for timescales in the range 125–360 min. At 65 min and 120 min timescales there is an overlap between the (rainfall average $PD \pm$ standard deviation) and the (runoff average $PD \pm$ standard deviation). The uncertainty range of RTS (see equation 3) is selected therefore as 60–125 min.

[32] As can be seen in Figures 7–9, the rainfall PD curve includes perturbations. The effect of these perturbations is to increase the range of the RTS values. For single events, this effect is more pronounced for perturbations at large timescales than at small timescales because of the exponential-like decay of the rainfall PD curve, which results in

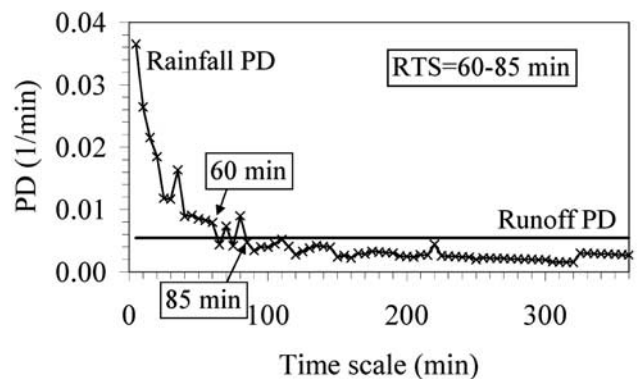


Figure 8. Same as Figure 7 for the Habel event of 22–23 January 1997. The RTS of the event is 60–85 min.

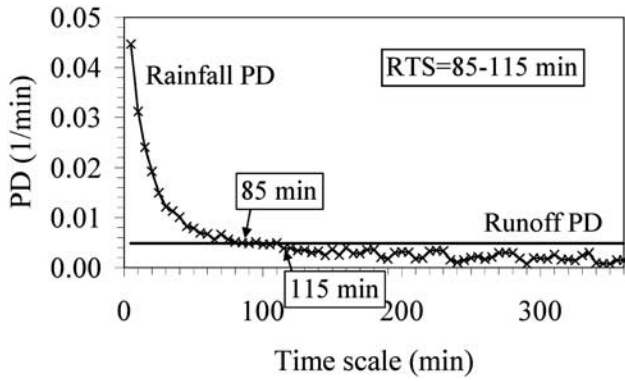


Figure 9. Same as Figure 7 for the Habel event of 21–24 February 1997. The RTS of the event is 85–115 min.

some asymmetry in the range of the RTS values. For a group of events, as a result of the averaging of the *PD* values, the perturbations are smaller (Figure 10) and this effect is reduced considerably.

[33] Comparing the RTS found for the individual events with the RTS found for the whole group (Figure 11) indicates that the group’s RTS range presents a reasonable limit to the individual events RTS. The variability of the RTS in this group is relatively low and the range of the

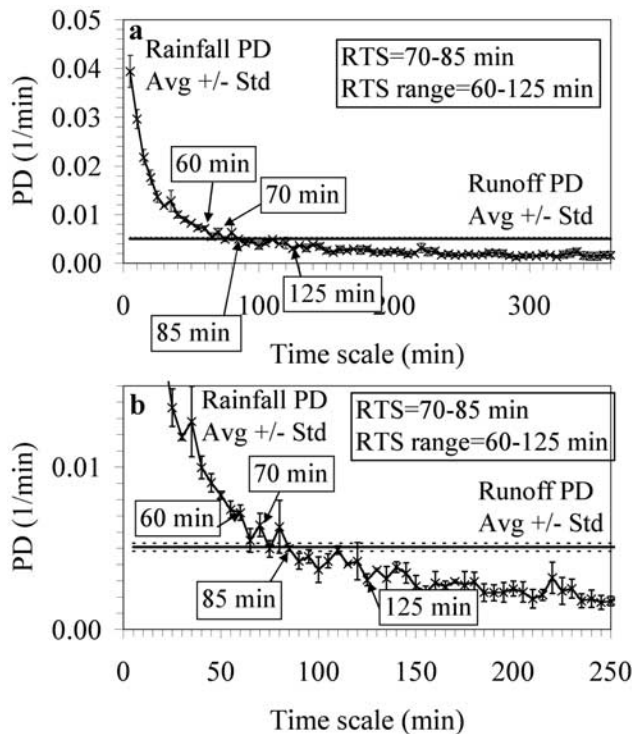


Figure 10. (a) Application of the RTS algorithm for the group of the three Habel events. (b) Enlarged view of crossover region. For each timescale in the range of 5–360 min (in 5 min steps), the average of the rainfall *PD* ± 1 standard deviation is presented (crosses for average and vertical lines for the bounds). The runoff average *PD* ± 1 standard deviation are drawn as lines (thick line for average and dashed lines for the bounds).

group RTS is relatively small. This implies that the RTS is stable for the group of events that were analyzed.

[34] The RTS parameter, according to the definition, is insensitive to the magnitude of rainfall and runoff graphs or to their shift in time. This property is very important knowing that large uncertainties exist in observed rainfall and runoff data. Following the RTS algorithm, it is clear that any linear change in magnitude as well as shift in time of data, will not affect the algorithm results. The only computational step of the algorithm during which some sensitivity to nonlinear changes might enter is the exclusion from the *PD* averaging of the low peaks (see step 6 in Appendix A).

[35] The robustness of the RTS is demonstrated here for the Habel catchment by applying linear and nonlinear changes in rainfall and runoff data and examining the effect of these changes on the determined RTS. The changes in data are generated by applying different Z-R calibration functions for calculating the radar rainfall intensities and by expressing runoff in terms of stage rather than discharge. Two Z-R transformation relations were tested: $Z = 200R^{1.6}$, $Z = 300R^{1.4}$. Each of these relations was applied with and without bias correction, which means correcting the radar rainfall by a factor such that the average radar rainfall above gauges equals the average gauges rainfall. Only slight differences in the estimated RTS are observed, as represented in Figure 12.

[36] Applying the RTS algorithm to runoff data presented as stage values rather than discharge, resulted in an RTS of 70–85 min with an uncertainty range of 60–125 min. This is the same as was found for discharge data.

5. Case Studies

5.1. Panama Catchment

[37] The RTS algorithm was applied to the Rio Pequeni catchment. The tested averaging timescales were in the range of 60–1200 min with a 60 min step (the measurement timescale). Figure 13 presents the RTS found for each one of the 190 events and for the whole group of events. Most of the RTS values found for the separate events lie in the range of 60–240 min, with a few cases (about 5%) having smaller or larger values. For the whole group of 190 events the RTS value of 120–180 min was found, which is also the RTS range. The RTS found is commensurate to the time to peak

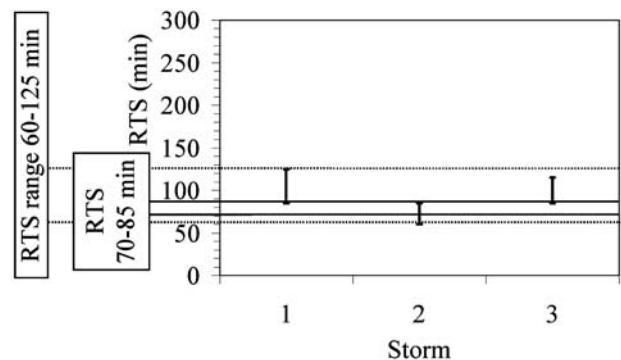


Figure 11. Comparison of the RTS found for the individual events (vertical bars) with the RTS value (solid horizontal lines) and uncertainty range (dashed horizontal lines) found for the whole group of events.

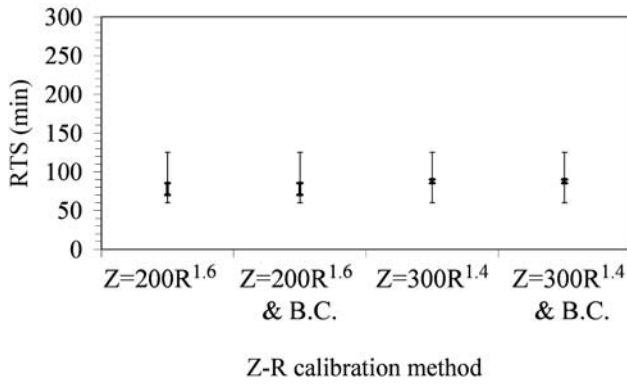


Figure 12. The RTS found for different Z-R calibration methods. Two power law equations with and without bias correction (B.C.) are tested. Thick lines represent the RTS value, and thin lines represent the RTS uncertainty range.

of the catchment’s unit hydrograph, which was estimated to be in the range of 150–180 min [Georgakakos *et al.*, 1999].

[38] For the event (4–13 January 1972), Figure 14 presents the rainfall at the smallest timescale available (1 hour, Figure 14a), rainfall averaged at a value within the RTS range (3 hours, Figure 14b) and rainfall averaged at timescale larger than the RTS (8 hours, Figure 14c) compared with the measured streamflow (Figure 14d). It is apparent that out of the three timescales, the RTS is the one for which the smoothness of the rainfall graph best fits the smoothness of the streamflow hydrograph.

[39] The Rio Pequeni rainfall-runoff data were analyzed to examine the effect of the peak discharge and number of peaks in the runoff hydrograph on the estimated RTS and its stability. Figure 15 presents the RTS as a function of peak discharge (Figure 15a) and of number of peaks (Figure 15b). The analysis includes all rainfall-runoff events with peak discharge larger than $20 \text{ m}^3 \text{ s}^{-1}$ (366 events). In general, it may be seen that for low flows as well as for hydrographs with a small number of peaks, the resulting RTS is spread over a large range of timescales. This range is smaller (i.e., the RTS becomes more stable) as the peak

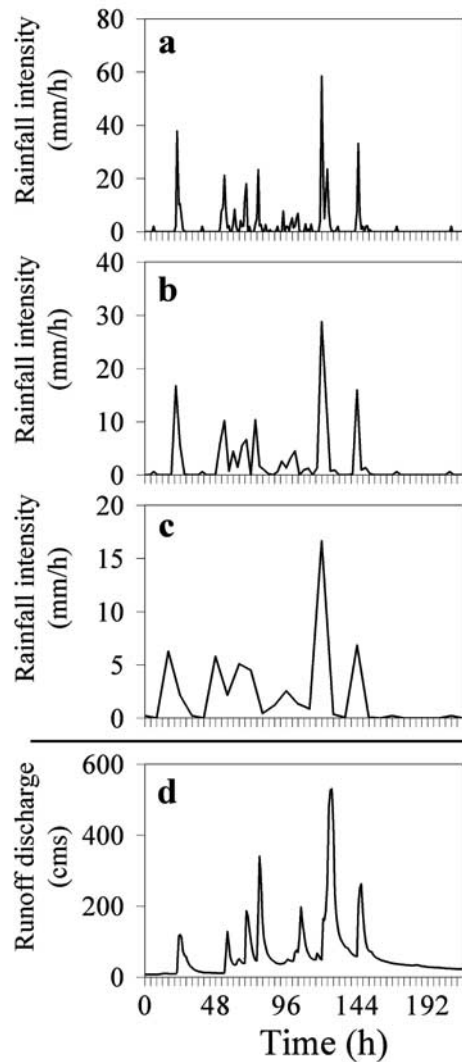


Figure 14. Rainfall and runoff graphs for the event of 4–13 January 1972 in the Rio Pequeni catchment. Rainfall graphs are catchment averaged at timescales of (a) 60 min, (b) 3 hours (RTS), and (c) 8 hours. (d) The runoff hydrograph.

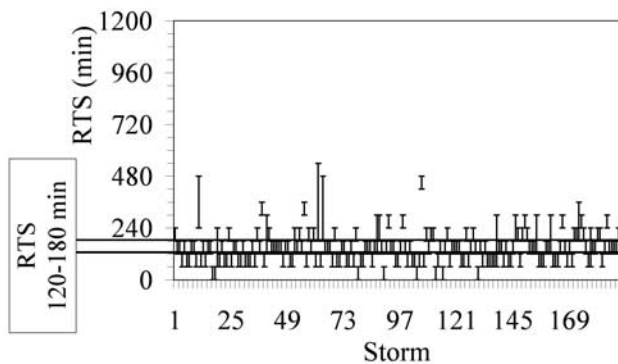


Figure 13. RTS found for each of the 190 rainfall-runoff events at which peak discharge is larger than $100 \text{ cm}^3 \text{ s}^{-1}$ in the Rio Pequeni catchment for the period 1972–1996. The RTS of the whole group (190 events) is 120–180 min (horizontal lines).

discharge increases and the number of peaks increases. The RTS of events with peak discharge higher than $100 \text{ m}^3 \text{ s}^{-1}$ and number of peaks higher than 12 is relatively stable and has a reasonably small range, as can be seen in Figure 15c.

[40] The number of events in a group needed to obtain a stable RTS value was also investigated using the Rio Pequeni data. Groups of different sizes in the range of 1–50 were selected randomly from the population of the 190 rainfall-runoff events with peak discharge larger than $100 \text{ m}^3 \text{ s}^{-1}$, and the RTS of each group was determined. For each group size, 50 groups were selected randomly. The spread of the RTS as a function of the group size is presented in Figure 16. If only one event is available, the RTS value for the single event can range from 0 (indicating value lower than the measurement scale, 60 min) to 540 min. For two to eight event groups, this range is decreased to 60–240 min. A narrower range of 60–180 min is found for nine and more events in a group. 50 events in a group are needed to get the same RTS that was found for the whole

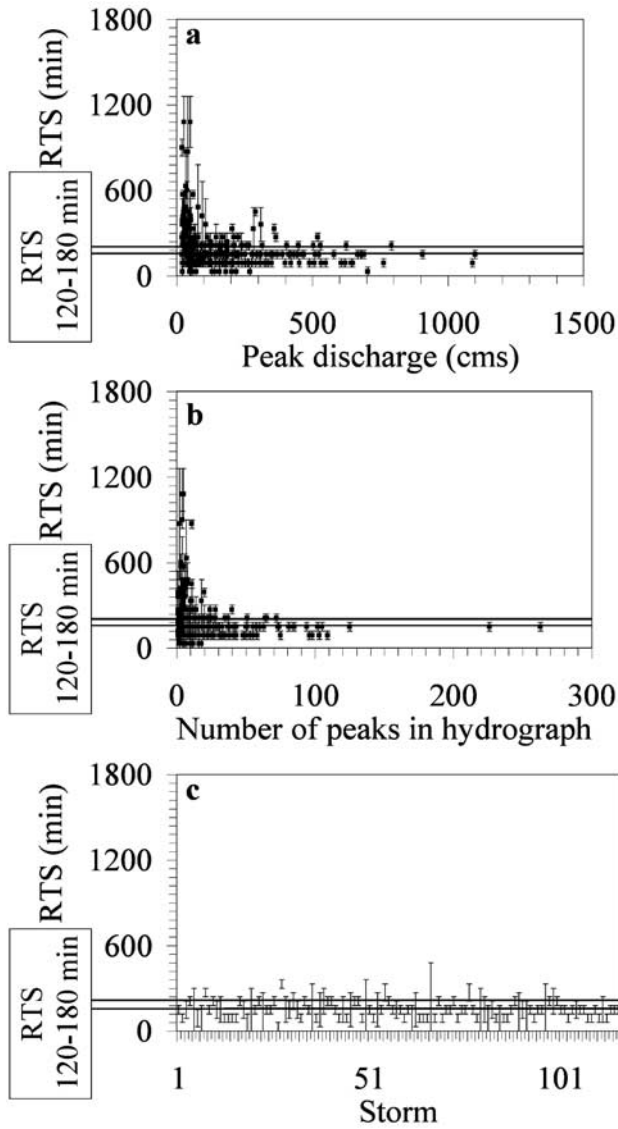


Figure 15. RTS (points present its median value, bars present its range) of rainfall-runoff events in the Rio Pequeni catchment as a function of (a) runoff peak discharge and (b) number of peaks in the runoff hydrographs. All rainfall-runoff events with peak discharge larger than 20 cm are analyzed. (c) The RTS of rainfall-runoff events with peak discharge larger than 100 cm and more than 12 peaks.

group of 190 events. Accepting the RTS values of 60–240 as a reasonable range around the “true” RTS of 120–180, the above results indicate that a relatively small number of events in a group (two events) are needed to obtain a stable RTS value. Obviously, this size may be dependent on catchment and climatic characteristics and probably a larger group of events is needed in regimes where there is a large variability in storm types.

5.2. Israeli Catchments

[41] Table 2 lists the events analyzed for each of the studied catchments. The RTS algorithm is applied for each event and for the group of events in each catchment. Table 3 summarizes the estimated RTS. Figure 17 presents for each catchment the comparison of the RTS of the individual

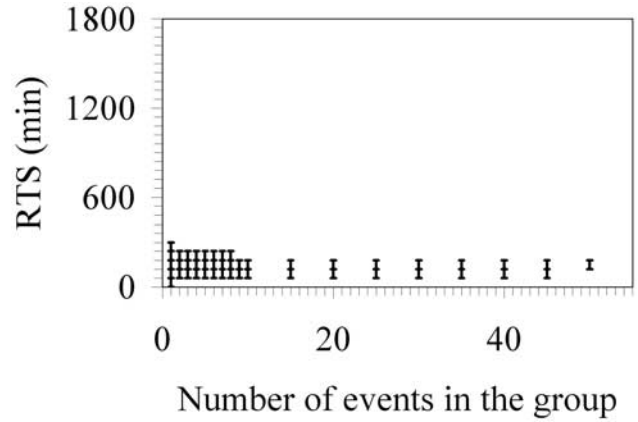


Figure 16. The span of RTS values (vertical axis) found for 50 groups of events of different sizes (horizontal axis), selected randomly from 190 events in the Rio Pequeni catchment.

events (vertical bars) with the RTS value (thick solid horizontal lines) and uncertainty range (dashed horizontal lines) of the group. A log scale was used for the time axis for clarity.

[42] For the Habel, Raanana and Ramon catchments the RTS found for the group of the analyzed events represents more or less an average RTS value, where the RTS uncertainty range reasonably limits the span of the individual RTS. For the Evtach catchment the individual RTS show higher variability and extend below and above the RTS uncertainty range of the whole group. One possible explanation for this is that the seven events that were analyzed represent two different responses of the catchment. Some of the events are from the 1991/1992 rainy season, which was

Table 3. Estimated RTS

Catchment	Event	RTS, min
Habel	17–20 Jan. 1996	85–125
Habel	22–23 Jan. 1997	60–85
Habel	21–24 Feb. 1997	85–115
Habel	RTS all storms	70–85
Habel	uncertainty range	60–125
Raanana	22 Feb. 1997	5–10
Raanana	17 March 1997	10–15
Raanana	30 Nov. 1997	<5
Raanana	24–25 Jan. 1998	<5
Raanana	17–19 March 1998	15–20
Raanana	29–30 March 1998	10–15
Raanana	RTS all storms	10–15
Raanana	Uncertainty range	5–15
Evtach	30 Nov. to 5 Dec. 1991	285–450
Evtach	11–16 Dec. 1991	215–350
Evtach	2–11 Feb. 1992	135–230
Evtach	22–28 Feb. 1992	100–125
Evtach	23–25 Nov. 1994	90–105
Evtach	2–6 Dec. 1994	65–80
Evtach	18–22 Dec. 1994	100–200
Evtach	RTS all storms	125–130
Evtach	uncertainty range	90–215
Ramon	13 Oct. 1991	45–85
Ramon	2–7 Nov. 1994	10–15
Ramon	8 Feb. 1996	35–40
Ramon	RTS all storms	30–35
Ramon	uncertainty range	10–85

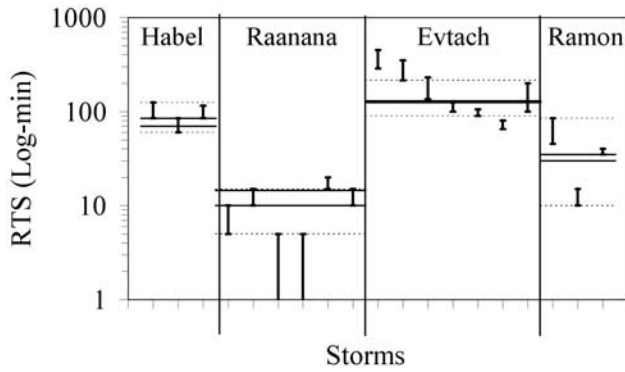


Figure 17. RTS values found for individual rainfall-runoff events (vertical bars) and for the group of events (horizontal lines) in four studied catchments in Israel. Dashed lines are the uncertainty range for the group. RTS represented in log scale for clarity.

an extremely wet winter in Israel with annual rainfall more than twice the mean annual value. The catchment was flooded over the stream banks several times as a result of the high rainfall amounts. In these events the catchment response time may be longer relative to the case of within-bank flows, as indicated by the high RTS found for the first three events with the highest peak discharges (the highest recorded for this catchment). Figure 17 suggests also that the large span of RTS for the individual high events is in the same order of magnitude (1–8 hours).

[43] For one event in each catchment Figures 18–21 show a comparison of the measured runoff hydrograph with the rainfall graph at three timescales: the smallest timescale (5 min), the RTS, and a timescale significantly larger than the RTS.

[44] Table 4 compares the RTS with the response timescale found for the same catchments of *Morin et al.* [2001] where an algorithm based on matching rainfall and runoff peaks was used. Generally, good agreement exists between the response timescales found by the two algorithms. For the Evtach catchment the difference between the results of the two algorithms is larger than for the other catchments, which can be explained by the types of events analyzed. Section 1.2 above considered the difference between the response timescale, which represents the integration time of the catchment, and the time of concentration, which is a combination of the integration time and translation time. Table 4 lists the estimated time of concentration parameters for each of the studied catchments. The first three values correspond (in their relative order) to RTS. For the Ramon catchment, however, the large time of concentration is in contrast to the small RTS value determined in the current study. This contradiction is not due to the formula used for estimating the time of concentration or the method used for determining the response timescale. Going back to the definition of concentration time, it takes several hours for a drop of water to travel more than 27 km (the length of Ramon's main channel) even if its velocity is high, while the small RTS value of the Ramon catchment relates probably to the rapid hydrological response and the limited coverage area of rainstorm that are known to characterize arid basins. It appears that these two timescales quantify

different aspects of the hydrological response, as suggested above.

6. Summary and Discussion

[45] The Response Timescale is a new parameter representing a range of characteristic times of the catchment hydrological response. It measures the amount of smoothing caused by the catchment response in transforming the rainfall into runoff. The procedure for estimating this measure is by comparing rainfall graphs averaged at different timescales with the runoff graph, and selecting the timescale at which the degree of smoothness of the two graphs is the same.

[46] The response timescale concept was first introduced by *Morin et al.* [2001] with a slightly different definition. The current paper outlines an objective automatic algorithm for estimating the RTS of a rainfall-runoff event or a group of events. For a group, the uncertainty range is also estimated. The RTS algorithm is applied to one catchment in Panama and to four catchments in Israel. The catchments are of sizes 10–150 km² and differ in their topography, land-use and climatic regime. The smallest RTS (10–15

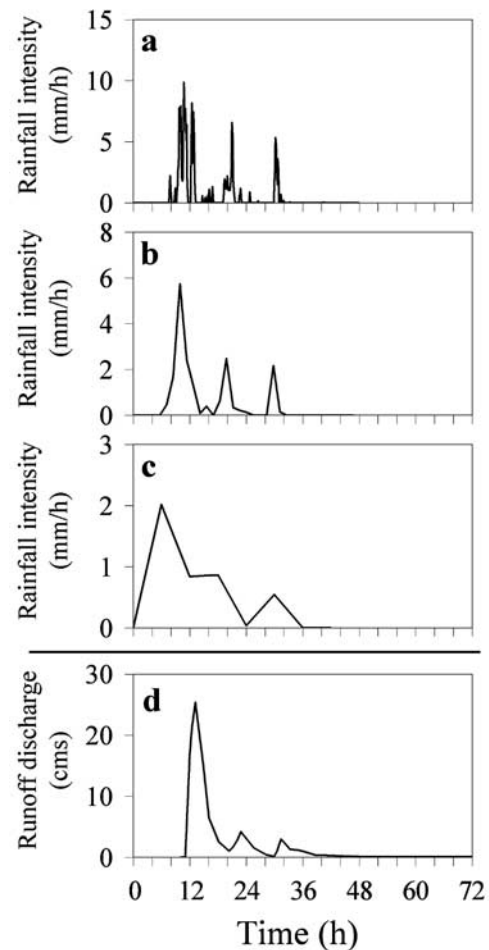


Figure 18. Rainfall and runoff graphs for the event of 22–23 January 1997 in the Habel catchment. Rainfall graphs are catchment averaged at timescales of (a) 5 min, (b) 85 min (RTS), and (c) 6 hours. (d) The runoff hydrograph.

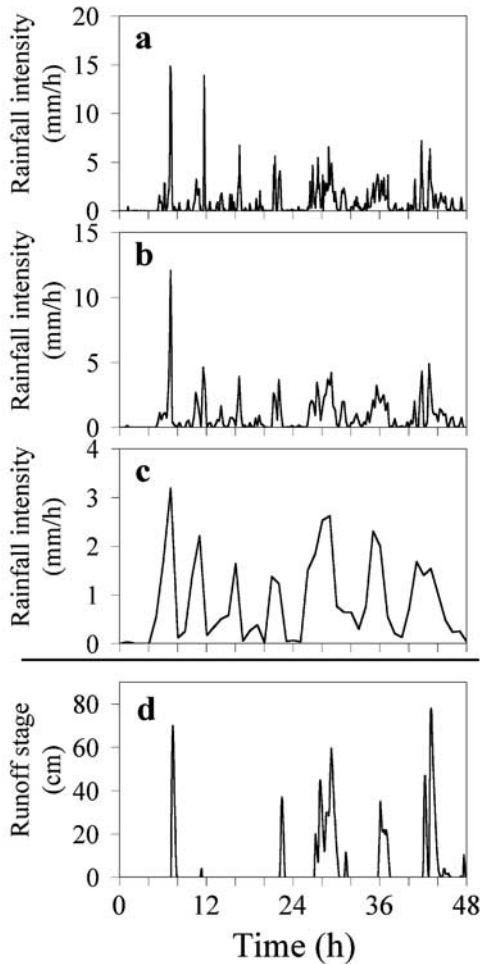


Figure 19. Rainfall and runoff graphs for the event of 21–23 January 1997 in the Raanana catchment. Rainfall graphs are catchment averaged at timescales of (a) 5 min, (b) 15 min (RTS), and (c) 60 min. (d) The runoff hydrograph.

min) was found for the urban 10 km² Raanana catchment. A relatively small RTS (30–35 min) was found also for the arid 98 km² Ramon catchment. The two rural catchments, Habel (24 km²) and Evtach (43 km²), were found to have RTS of 70–85 min and 125–130 min, respectively. The RTS of the forested, mountainous, 133 km² Rio Pequeni catchment is 120–180 min. These RTS values indicate that, as expected, the urban and arid catchments have faster hydrological response compared to the rural and forested catchments. The RTS algorithm successfully captures this inherent difference in catchment response.

[47] In general, all the RTS values found are reasonably stable. It was shown that stable RTS values are more likely to be estimated for high flows with multiple peaks. For the Ramon catchment, typical to arid regions, the flow hydrograph often contains a single peak. Still, based on three rainfall-runoff events, the RTS value of 30–35 min was estimated using the automatic objective algorithm. This is the same value as was estimated subjectively for the Ramon catchment of *Morin et al.* [2001]. It is interesting to note that multiple peak hydrographs that were found to be better for determining the RTS are considered less appropriate for estimating other time parameters such as time of concen-

tration and lag time. Single peak hydrographs are usually preferred in estimating these latter parameters.

[48] There are some benefits in the proposed approach for estimating the characteristic time of the catchment hydrological response. First, the RTS is a model-free parameter, because no assumption is made on the rainfall-runoff transformation function. Furthermore, rainfall data can be used directly in the analysis rather than rainfall excess as in the case for example of unit hydrograph estimation. Second, the RTS is a magnitude-independent parameter, because it refers only to the smoothness of the rainfall and runoff graphs and not to their magnitude. Both types of data, the catchment averaged rainfall (based on radar or rain gauges data) and the runoff, are known to include errors; the ability to tolerate these errors is a major advantage. The algorithm presented in this paper was shown to be robust to data magnitude errors for one case study. Although it does not tolerate completely nonlinear errors in the data, its sensitivity to this type of error is small. In addition, determining the RTS parameter does not involve matching the rainfall and runoff time series and thus timing errors can also be tolerated. These errors are typical to data generated by mechanical gauges, but are also found in digital data. The

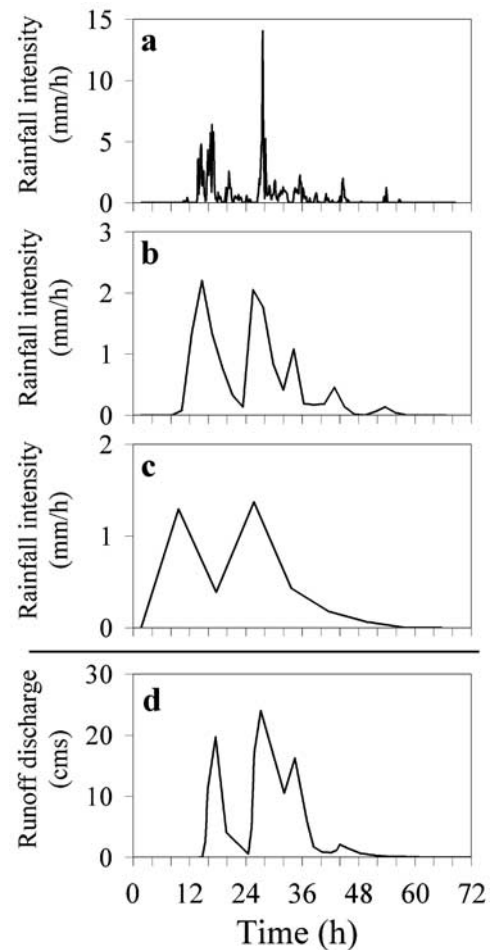


Figure 20. Rainfall and runoff graphs for the event of 23–26 November 1994 in the Evtach catchment. Rainfall graphs are catchment averaged at timescales of (a) 5 min, (b) 130 min (RTS), and (c) 8 hours. (d) The runoff hydrograph.

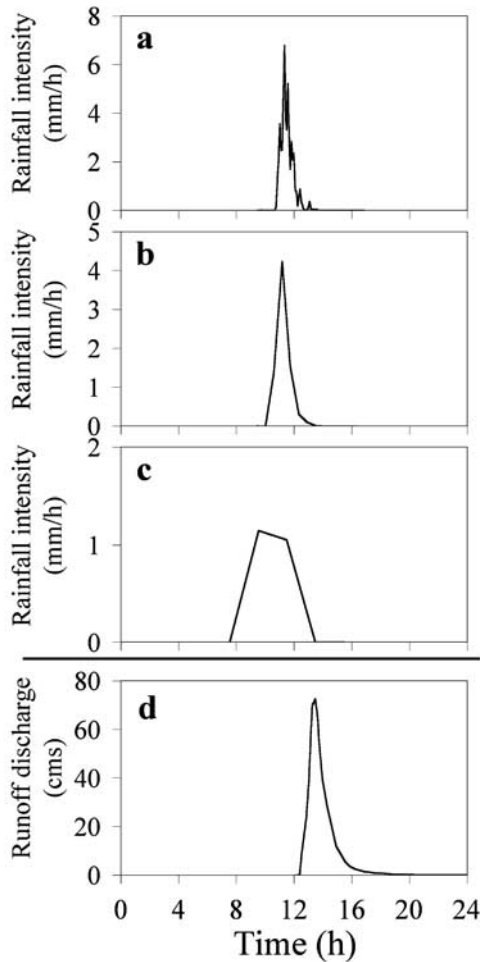


Figure 21. Rainfall and runoff graphs for the event of 8 February 1996 in the Ramon catchment. Rainfall graphs are catchment averaged at timescales of (a) 5 min, (b) 35 min (RTS), and (c) 2 hours. (d) The runoff hydrograph.

timing errors to which the procedure is not sensitive are shifts in time. Shrinking or stretching the time axis, on the other hand, might affect the resulting RTS.

[49] The main limitation in the approach is that it is based on observed rainfall and runoff data, and thus it can be applied only to gauged catchments. Further investigation is required to relate the RTS to catchment characteristics and make it applicable to ungauged catchments as well.

[50] We suggest associating the response timescale with the integration time of the catchment, which is one of two major time characteristics of the hydrological response, where the second is the translation time (see section 1.2). In this context, the stability and the magnitude insensitivity of the RTS should be clarified. The range of the RTS values represents the mean response, over several events, of the catchment. The results shown here indicate that the integration time for individual events in a catchment varies somewhat and is not always exactly the same, but deviations from the mean response are not large. Antecedent conditions, storm properties in general and rainfall magnitude in particular have a relatively small effect on the integration time, at least for the cases studied. This conclusion is not obvious and its generality should be confirmed by additional studies.

[51] The factors listed above can have a significant effect on other features of the runoff hydrograph. For example, consider runoff hydrographs generated by the same rainfall but with different antecedent soil moisture. The hydrographs will probably differ in their magnitude and in the time to flow initiation; however, according to our results, the smoothness of the hydrographs, or more specifically the *PD* of the runoff hydrographs, will probably be very similar. The *PD* is derived for times when flow exists, and very small runoff peaks are eliminated from the analyses using an automatically defined noise parameter. As another example, it is probable that different locations of storm centers will significantly affect the translation time, which we associate with the lag time parameter, but they will not necessarily affect the integration time. As stated above, additional analyses are still needed to examine how general these results are and to understand their physical causes.

[52] We suggested that the difference between the RTS and the lag time parameters is that the first is associated with the integration time and the second with the translation time. The time of concentration is a combination of these two times. Although the two types of time characteristics may be related to each other, in some cases, a significant difference can exist between them. Consider for example the arid Ramon catchment. As demonstrated in Figure 21, the time interval between the rainfall peak and the runoff peak is more than 2 hours, but an integration time of 2 hours (Figure 21c) seems too large in this case. So, in this example, the lag time and the time of concentration, affected by the long distance of travel in the channel (27 km), are relatively large (see Table 4), but the appropriate integration time is significantly shorter. The ability to determine each type of timescale separately can be important for different hydrological applications. For example, for estimating flood frequency, time parameters are needed to represent the critical durations of flood-producing rainfall. Several studies suggested using the lag time parameter for this purpose [e.g., Bell and Om Kar, 1969; Iacobellis and Fiorentino, 2000]. However, as discussed above, it is possible to find relatively large lag times in catchments that respond to short rainfall durations (especially in arid regions). The current study suggests that the catchment RTS maybe a more appropriate time parameter in these applications. Further analysis is necessary to confirm this conjecture.

[53] An additional advantage of the RTS is in its insensitivity to magnitude. This information combined with other

Table 4. RTS of the Israeli Studied Catchments Based on Two Algorithms and Time of Concentration

Catchment	RTS, min	Uncertainty Range, min	T_s^* , min ^a	T_s^* Range, min ^a	Time of Concentration, min ^b
Habel	70–85	60–125	90	60–150	150
Raanana	10–15	5–15	15	15–20	80
Evtach	125–130	90–215	180	150–210	250
Ramon	30–35	10–85	30	20–40	350

^a The response timescale and its uncertainty range based on the algorithm presented by Morin et al. [2001].

^b Based on formula used by the Soil Conservation Division in the Israeli Ministry of Agriculture and Rural Development [Garti et al., 1998].

measures, for example one that is sensitive to magnitude but not to smoothness, generates a set of orthogonal parameters that can serve in the process of hydrological model calibration and evaluation. Currently, model performance is evaluated using functions that cannot separate between errors in magnitude and other types of error such as in the hydrograph shape. An example of this possibility is shown by Shamir *et al.* [2002].

[54] It is interesting to consider also the relationships of the RTS to the unit hydrograph. For the Panama catchment, for which a unit hydrograph is available, the estimated RTS is similar to the estimated time to peak. If that will be found to be true in the general case, it implies that the RTS represents a range of times to peak, which relaxes the linear assumption of unit hydrograph theory. Compared to the time to peak of the unit hydrograph, the RTS is easier to determine, because it is based on the actual rainfall rather than on excess rainfall, which requires estimation of groundwater and evapotranspiration losses. A possible application of this result, if it is shown to be true in general, is incorporating the RTS parameter in estimating an empirical unit hydrograph. Of course, additional information is needed about other features of the unit hydrograph such as its peak magnitude.

7. Concluding Remarks

[55] The response timescale represents a measure of the characteristic time of the catchment hydrological response. It quantifies the amount of smoothness performed on the input when transformed into output by identifying the equivalent averaging that has to be applied to the rainfall such that it will have the same smoothness as the runoff. The smoothness of the rainfall and runoff graphs is represented by their peak density, which is defined in the paper. The main advantages in the response timescale approach are that nothing is assumed about the transformation of rainfall into runoff and, in addition, this measure appears robust against measurement errors.

[56] An objective, automatic, observations-based algorithm is described in the paper that determines the response timescale of event or a group of events. For a group, an uncertainty range is also calculated. The algorithm was applied to a catchment in Panama and to four catchments in Israel. In all cases, relatively stable values of response timescale were found. It is concluded that, at least for the case studies, the response timescale is an intrinsic and stable characteristic of the catchment.

[57] It is suggested that the response timescale is different from the lag time and time of concentration parameters. Lag time is a measure of the time of flow along the entire length of the catchment, while the response timescale measures the integration time. Time of concentration is a combination of these two. The response timescale maybe appropriate for use in hydrological applications such as flood frequency estimation.

[58] Further research should concentrate on determining the relationship of the response timescale, as defined herein, to catchment characteristics using either observed data from well instrumented catchments or extensive simulations of well verified hydrologic rainfall-runoff models.

[59] The concept of the RTS is particularly suitable when radar rainfall data are available, which are characterized by

(1) spatial coverage that provides integration of the rainfall event over the catchment, (2) good time resolution, and (3) difficulties in determining the absolute magnitude of the rainfall intensities. The result is a hyetograph that has good “shape definition” of the rainfall event over the catchment, but not as good “magnitude definition”. The RTS exploits the hyetograph shape and is insensitive to magnitude. It is also insensitive to matching the absolute timescales of the rainfall and runoff events.

Appendix A

[60] The following are the steps of the algorithm for determining the Peak Density (*PD*) of a time series $\{y(n)\}_{n=1}^N$ representing values of a graph at equal time intervals Δt .

1. Points are marked as increases or decreases. Given a noise parameter *eps*, each point in the graph is marked by +1 (“real increase”), if $y(n) - \text{MinBase} > \text{eps}$, -1 (“real decrease”), if $\text{MaxBase} - y(n) > \text{eps}$, 0 (“not clear”) otherwise. *MinBase* and *MaxBase* are reference values that are defined for each point *n* in the following way: if the preceding point, $n - 1$, is signed by +1 or -1, then the two reference values are equal to $y(n - 1)$. Otherwise, *MinBase* is the minimum value of all the successively preceding points that have zero sign (i.e., $\{y(k)\}_{k=l}^n = 0$, such that the sign of all points $k = l..n - 1$ is zero and the sign of point $l - 1$ is +1 or -1, or $l = 1$) and *MaxBase* is the maximum value of the same group. Initially, *MinBase* and *MaxBase* are equal to $y(1)$. Different values are assigned automatically in the procedure to the *eps* parameter as described in step 6.

2. Small (“unclear”) increases/decreases that are adjacent to real increases/decreases are marked accordingly. For each point that is marked by +1, all the successively preceding points and the successively following points *k* that are marked by zero and are increase (i.e., $y(k) > y(k - 1)$), their sign is changed to +1. In the same way, for each point marked by -1, all the successively preceding and following points that have sign zero and are decrease; their sign is changed to -1.

3. Peaks are identified. The time series is separated into individual peaks according to the following rules. A peak is a series of points $\{y(k)\}_{k=l}^m$ such that point *l* is marked by +1, point *m* is marked by -1, and there are no $l \leq i < j \leq m$ such that the sign of point *i* is -1 and the sign of point *j* is +1. In other words, a peak is a series of +1 points followed by -1 points, possibly with zeros in between. The first point should be the smallest possible such that the above conditions hold. Thus there is no $i < l$ such that the mark of point *i* is +1 and the mark of all the points in between *i* and *l* is zero. In the same way, the last point of the peak should be the largest possible that the above conditions hold.

4. Durations of peak rising limbs are identified. For each peak $\{y(k)\}_{k=l}^m$, let *r* be the point of maximum value ($l \leq r \leq m$, $y(k) \leq y(r)$ for each $l \leq k \leq m$). The duration of the rising limb of the peak is defined as: $(r - l + 1) \times \Delta t$.

5. The peak density of the graph for a given noise parameter is calculate. *PD*, the peak density of the graph represented by the time series $\{y(n)\}_{n=1}^N$ is defined as the ratio of *TPN*, the number of peaks in the time series, to *TRLD*, the sum of durations of rising limbs for all these peaks. The *PD* depends on the noise parameter *eps*.

6. The graph peak density is calculated. Steps 1–5 are first applied with the noise parameter $eps = 0$. The peaks of the graph are identified and the PD is calculated. If the graph contains more than one peak, the eps value is set to be the height of the smallest peak, and steps 1–5 are applied again with the new noise parameter. This process is stopped when the graph contains one peak only. The result is a set of PD values for increasing values of eps . The final PD of the graph is taken as the average of all the PD values calculated with noise parameters larger than 10 percent of the largest one (i.e., the eps with which only one peak was calculated in the graph).

[61] **Acknowledgments.** We thank two anonymous reviewers of the paper and the associate editor for their helpful recommendations. For the catchments in Israel, radar data were provided by E.M.S (Mekorot), runoff data were provided by the Hydrological Service of Israel, and rain gauge data were provided by the Israel Meteorological Service. G.I.S analysis was carried out using the G.I.S Laboratory of the Hebrew University. For the Rio Pequeni catchment, hourly rain gauge and streamflow data were provided by the Panama Canal Authority. This project was funded by grants from the United States-Israel Binational Science Foundation (grant 97-00026) to the Hebrew University in Israel and the Hydrologic Research Center in the USA. Additional funding was provided by the Jewish National Fund.

References

- Austin, P., Relation between measured radar reflectivity and surface rainfall, *Mon. Weather Rev.*, 115, 1053–1071, 1987.
- Bell, F. C., and S. Om Kar, Characteristic response times in design flood estimation, *J. Hydrol.*, 8, 173–196, 1969.
- Ben-Zvi, A., Runoff peaks from two-dimensional laboratory watersheds, *J. Hydrol.*, 68, 115–139, 1984.
- Caroni, E., R. Rosso, and F. Siccardi, Nonlinearity and time-variance of the hydrological response of a small mountain creek, in *Scale Problems in Hydrology*, edited by V. K. Gupta, I. Rodriguez-Iturbe, and E. Wood, pp. 19–37, D. Reidel, Norwell, Mass., 1986.
- Dan, Y., and Z. Raz, Map of Israel soil groups 1:250,000, Soil Conserv. Div., Minist. of Agric., Tel-Aviv, Israel, 1970.
- Garti, R., M. Getker, and S. Arbel, Peak discharges and runoff volumes in sub-basins in winter 1996/97 (in Hebrew), *Rep. M-58*, Soil Erosion Res. Stn., Soil Conserv. Div., Minist. of Agric. and Rural Dev., Tel-Aviv, Israel, 1998.
- Georgakakos, K. P., J. A. Sperflage, D. Tsintikidis, T. M. Carpenter, W. F. Krajewski, and A. Kruger, Design and tests of an integrated hydrometeorological forecast system for the operational estimation and forecasting of rainfall and streamflow in the mountainous Panama Canal watershed, *HRC Tech Rep. 2*, 143 pp., Hydrol. Res. Cent., San Diego, Calif., 1999.
- Horton, R. E., Erosional development of streams and their drainage basins: Hydrophysical approach to quantitative morphology, *Bull. Geol. Soc. Am.*, 56, 275–370, 1945.
- Iacobellis, V., and M. Fiorentino, Derived distribution of floods based on concept of partial area coverage with a climatic appeal, *Water Resour. Res.*, 36(2), 469–482, 2000.
- Kirpich, T. P., Time of concentration of small agricultural watersheds, *Civ. Eng.*, 10(6), 362, 1940.
- Kuichling, E., The relation between the rainfall and the discharge of sewers in populous districts, *Trans. Am. Soc. Civ. Eng.*, 20, 1–60, 1889.
- Marshall, J. S., and W. M. Palmer, The distribution of raindrops with size, *J. Meteorol.*, 5, 165–166, 1948.
- Michaud, J. D., K. K. Hirschboeck, and M. Winchell, Regional variations in small-basin floods in the United States, *Water Resour. Res.*, 37(5), 1405–1416, 2001.
- Morin, E., Y. Enzel, U. Shamir, and R. Garti, The characteristic time scale for basin hydrological response using radar data, *J. Hydrol.*, 252, 85–99, 2001.
- Nash, J. E., Systematic determination of unit hydrograph parameters, *J. Geophys. Res.*, 64(1), 111–115, 1959.
- Overton, D. E., and M. E. Meadows, *Stormwater Modeling*, Academic, San Diego, Calif., 1976.
- Robinson, J. S., and M. Sivapalan, Temporal scales and hydrological regimes: Implications for flood frequency scaling, *Water Resour. Res.*, 33(12), 2981–2999, 1997.
- Rodriguez-Iturbe, I., and J. B. Valdes, The geomorphic structure of the hydrologic response, *Water Resour. Res.*, 15(6), 1409–1420, 1979.
- Shamir, E., E. Morin, B. Imam, and S. Sorooshian, Incorporating hydrograph shape descriptors in model parameter estimation, paper presented at Second Federal Interagency Hydrologic Modeling Conference, Subcomm. on Hydrol., Las Vegas, Nev., 28 July to August 2002.
- Simas, M. J., and R. H. Hawkins, Lag time characteristics for small watersheds in the U.S., paper presented at Conference of American Society of Civil Engineers, Am. Soc. of Civ. Eng., Memphis, Tenn., August, 1998.
- Singh, V. P., Derivation of the time of concentration, *J. Hydrol.*, 30, 147–165, 1976.
- Singh, V. P., *Elementary Hydrology*, 972 pp., Prentice-Hall, Old Tappan, N. J., 1992.
- Soil Conservation Service, Hydrology, in *SCS National Engineering Handbook*, U.S. Dep. of Agric., Washington, D. C., 1972.
- Soil Conservation Service, Urban hydrology for small watersheds, *Tech. Release 55*, U.S. Dep. of Agric., Washington, D. C., 1975.
- Y. Enzel, Institute of Earth Sciences, Hebrew University of Jerusalem, Jerusalem 91904, Israel.
- R. Garti, Soil Erosion Research Station, Emek Hefer 40250, Israel.
- K. P. Georgakakos, Hydrologic Research Center, 12780 High Bluff Drive, Suite 250, San Diego, CA 92130, USA.
- E. Morin, Department of Hydrology and Water Resources, University of Arizona, 1133 East North Campus Drive, Tucson, AZ 85721, USA. (morine@hwr.arizona.edu)
- U. Shamir, Faculty of Civil Engineering and Stephen and Nancy Grand Water Research Institute, Technion, Haifa 32000, Israel.